
Learning-Based TSP-Solvers Tend to Be Overly Greedy

Xiayang Li^{1,2} and Shihua Zhang^{1,2,*}

¹Academy of Mathematics and Systems Science, Chinese Academy of Sciences

²School of Mathematics Sciences, University of Chinese Academy of Sciences

*Corresponding Author

Abstract

Deep learning has shown significant potential in solving combinatorial optimization problems such as the Euclidean traveling salesman problem (TSP). However, most training and test instances for existing TSP algorithms are generated randomly from specific distributions like uniform distribution. This has led to a lack of analysis and understanding of the performance of deep learning algorithms in out-of-distribution (OOD) generalization scenarios, which has a close relationship with the worst-case performance in the combinatorial optimization field. For data-driven algorithms, the statistical properties of randomly generated datasets are critical. This study constructs a statistical measure called *nearest-neighbor density* to verify the asymptotic properties of randomly generated datasets and reveal the greedy behavior of learning-based solvers, i.e., always choosing the nearest neighbor nodes to construct the solution path. Based on this statistical measure, we develop interpretable data augmentation methods that rely on distribution shifts or instance perturbations and validate that the performance of the learning-based solvers degenerates much on such augmented data. Moreover, fine-tuning learning-based solvers with augmented data further enhances their generalization abilities. In short, we decipher the limitations of learning-based TSP solvers tending to be overly greedy, which may have profound implications for AI-empowered combinatorial optimization solvers.

1 Introduction

Traveling Salesman Problem (TSP) is a critical and widely applied combinatorial optimization problem. It involves finding the shortest possible route that visits a given set of cities exactly once and returns to the origin city. Due to its NP-hard nature, TSP is a central problem in optimization theory with numerous practical applications in logistics^[5], routing^[24], manufacturing^[4], and even circuit design^[23].

Previous studies have developed various exact and heuristic methods to tackle TSP, including dynamic programming^[13], branch-and-bound^[30], and genetic algorithms^[20]. However, due to the combinatorial explosion of possible solutions as the number of cities increases, finding the optimal solution becomes computationally infeasible for large instances. This has led to significant interest in approximation algorithms and learning-based approaches that can offer near-optimal solutions in a reasonable amount of time. Deep learning techniques^[21] provide a novel ‘data-driven’ approach to problem-solving, enabling researchers to address challenges from computational complexity more effectively. The learning-based algorithms can be divided into two main categories^[28]: i) Learning-based end-to-end algorithms, especially the end-to-end construction algorithm; ii) Hybrid algorithms combining deep learning with heuristic algorithms. This study investigates the potential biases in

solving TSP using deep learning solvers. Given the difficulty in isolating the sources of bias in the latter category, this paper focuses on the study of end-to-end construction algorithms.

End-to-end construction algorithms employ neural networks to learn construction heuristics and construct solutions from scratch, exhibiting rapid solving speed. The algorithms typically utilize an encoder-decoder structure. The encoder generates embeddings for nodes, while the decoder computes the probability distribution of candidate nodes based on the information of encoders. Ptr-Net^[29] is a typical representative. However, due to the limitations of supervised learning, the solution quality is often low. The algorithms developed based on Ptr-Net^[14,16,18,34,36] utilize reinforcement learning algorithms to train models for improving solution quality.

However, due to their data-driven nature, some challenges remain. The existing literature fails to solve TSP instances when training and test data have different distributions. One perspective is the difficulty of scale generalization, which manifests in the larger scale of the test instances. In this paper, we take an orthogonal direction by considering the generalization of algorithms on instances of the same size but having different distributions. Researchers typically train neural network solvers using reinforcement learning methods with random datasets of sizes TSP20/50/100^[28] generated with node coordinates in the unit square $[0, 1]^2$. When tested on a dataset generated with a uniform distribution, the neural solver typically performs well. However, we are unsure whether learning-based solvers would still work well on some structures, which hinders the solver’s application in real-world problems. At the same time, analyzing instances of combinatorial optimization problems can effectively identify bottlenecks in learning models and algorithms. With the support of scaling laws^[17], the performance of the large model has improved significantly with size. However, as data resources become increasingly scarce, the importance of data quality in model training is becoming more pronounced^[33]. Delving into and analyzing combinatorial optimization instances with numerous corner cases will help drive the transformation and development of data-driven approaches.

In this paper, we analyze the (implicit) statistical properties of datasets generated with the uniform distribution, explain the potential implicit biases in the algorithm called greedy behavior, i.e., always choosing the nearest nodes for the solution construction, and demonstrate that such biases exist. On the other hand, we develop a data augmentation method to improve model robustness. However, for learning-based solvers, can data augmentation truly elevate them to the level of a general-purpose solver^[32]? This is one of the questions we aim to answer here.

2 Overview

In this study, we construct a statistical measure called the *nearest-neighbor density* and validate the greedy behavior of the learning-based solvers introduced by data sampling from uniform or normal distributions and real-world city instances (**Fig. 1a,b**). We provide the asymptotic lower bound of the nearest-neighbor density under uniform distribution and formulate a mathematical conjecture. This conjecture could be a significant open problem in probability theory, graph theory, and combinatorial optimization. We leverage the nearest-neighbor density to develop augmented instances for TSP deep-learning solvers. These instances are constructed based on distributional shifts and node perturbations. We verify that these more diverse instances effectively interfere with learning-based solvers. By using these instances as augmented TSP instances, we fine-tune some base solvers^[14,16,19,34,36] and confirm a substantial improvement in the generalization performance. Although our data augmentation method based on nearest-neighbor density can improve the learning-based solvers’ performance, it is not complete. Unless NP = co-NP, there does not exist an effective and complete data augmentation method. Also, we introduce the concept of efficient algorithm covering and demonstrate that unless NP = P, there is no solution to obtain a general-purpose solver by integrating polynomially many (biased) algorithms.

3 The nearest-neighbor density

3.1 From the nearest-neighbor algorithm to the nearest-neighbor density

Given a set of cities $\{c_1, c_2, \dots, c_N\}$ and a distances $d(c_i, c_j)$ for each pair of distinct cities $\{c_i, c_j\}$, the goal of TSP is to find an ordering π of the cities that minimizes the quantity:

$$\sum_{i=1}^{N-1} d(c_{\pi(i)}, c_{\pi(i+1)}) + d(c_{\pi(N)}, c_{\pi(1)}) \quad (1)$$

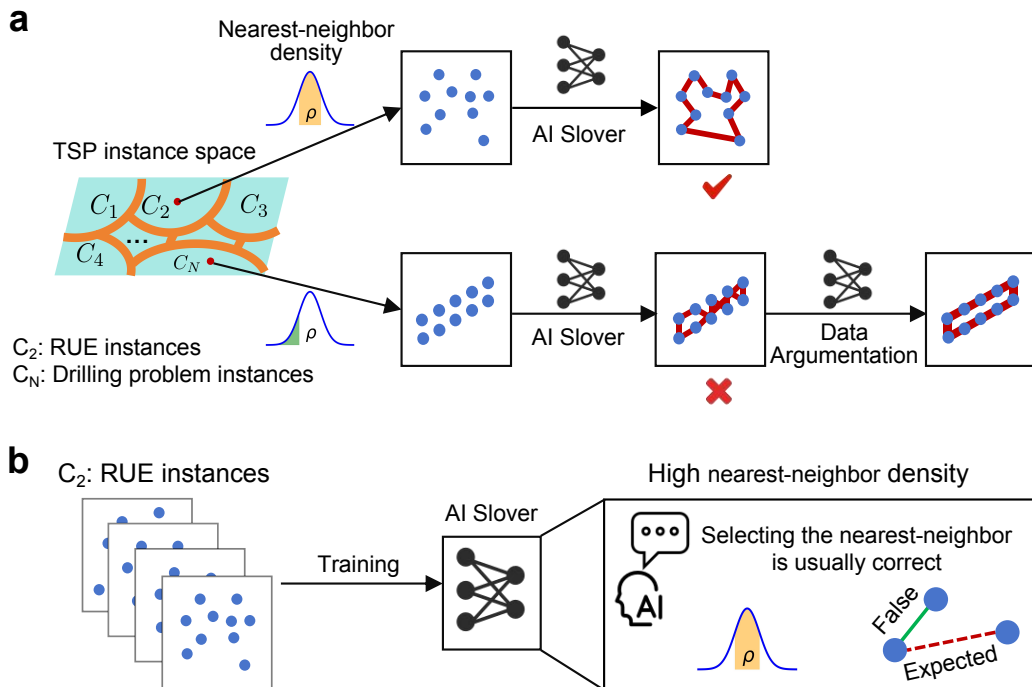


Figure 1: **(a)** Using random uniform Euclidean (RUE) data for model training may lead to algorithmic bias. In other words, the algorithm cannot guarantee that data from all structures are effective at the same scale. We can explicitly mine instances that cause the algorithm to fail using the nearest-neighbor density measure. **(b)** The mechanism behind the bias introduced by datasets. Specifically, the model is trained on a dataset generated from a uniform distribution, which has a high nearest-neighbor density characteristic. As a result, the model may incorrectly assume a causal relationship between nearest-neighbor density and the solution.

This quantity is referred to as the tour length that a salesman would make when visiting the cities in the order specified by the permutation, returning to the initial one at the end. We concentrate on the symmetric TSP on the two-dimensional Euclidean plane, satisfying the triangle inequality.

The most natural heuristic or greedy strategy for TSP is the famous nearest-neighbor algorithm (NN). It always selects the nearest as-yet-unvisited location as the next node. Due to its poor performance, it is generally not used for TSP. There is only a theoretical guarantee that $\frac{NN(I)}{OPT(I)} \leq 0.5(\lceil \log_2 N \rceil + 1)$, and no substantially better guarantee is possible as there are instances for which ratio grows as $\Theta(\log N)^{126}$. In this paper, we consider the question from another view: **For general instances, what proportion do the nearest-neighbor nodes or edges occupy in the optimal solution?** We generate instances uniformly distributed in a two-dimensional Euclidean plane with node sizes of 50, 100, and 200 and plot the images of the nearest-neighbor edges and the optimal solution (**Fig. 2**). We found that the proportion of nearest-neighbor edges in the optimal solution is very high. For example, in the instance with 50 nodes, only five nearest-neighbor edges do not appear in the optimal solution.

Here, we propose a statistical measure that characterizes the proportion of nearest-neighbor edges in the optimal solution. We introduce a node-based nearest-neighbor density considering that the algorithm progressively selects the next node to visit during its execution.

Definition 1 (The Nearest-Neighbor Density). *For a TSP instance $G = (V, E, d)$, where V is the set of vertices with the size of n , E is the set of edges with the size of m and d is the weight of the edges, i.e., the Euclidean distance between two points in the two-dimensional Euclidean plane. Given the optimal tour τ^* found, we denote $\mathcal{N}(c_i)$ and $\mathcal{N}'(c_i)$ as the set of the nearest-neighbors of c_i on G*

and on τ^* , respectively. The nearest-neighbor density ρ_n^* is calculated as follows:

$$\rho_n^* = \sum_{c_i \in V} \frac{|\mathcal{N}(c_i) \cap \mathcal{N}'(c_i)|}{|\mathcal{N}(c_i)| \cdot n}. \quad (2)$$

Remark 1. For a continuous probability distribution sampling dataset, the set of points where a given node c has more than one nearest-neighbor, i.e., two or more nodes are equidistant from c constitute a null set. In this case, the calculation of ρ_n simplifies to a specific form:

$$\rho_n^* = \sum_{c_i \in V} \frac{I(c_i)}{n},$$

where $I(c_i) = \begin{cases} 1, & c_i \text{ is adjacent to } c \in \mathcal{N}(c_i) \text{ on } \tau^*, \\ 0, & \text{others.} \end{cases}$ However, in some real-world or synthetic datasets, a node may have multiple nearest neighbors. Therefore, it is necessary to use Equation 2 for calculation. For specific examples, refer to those provided in TSPLIB.

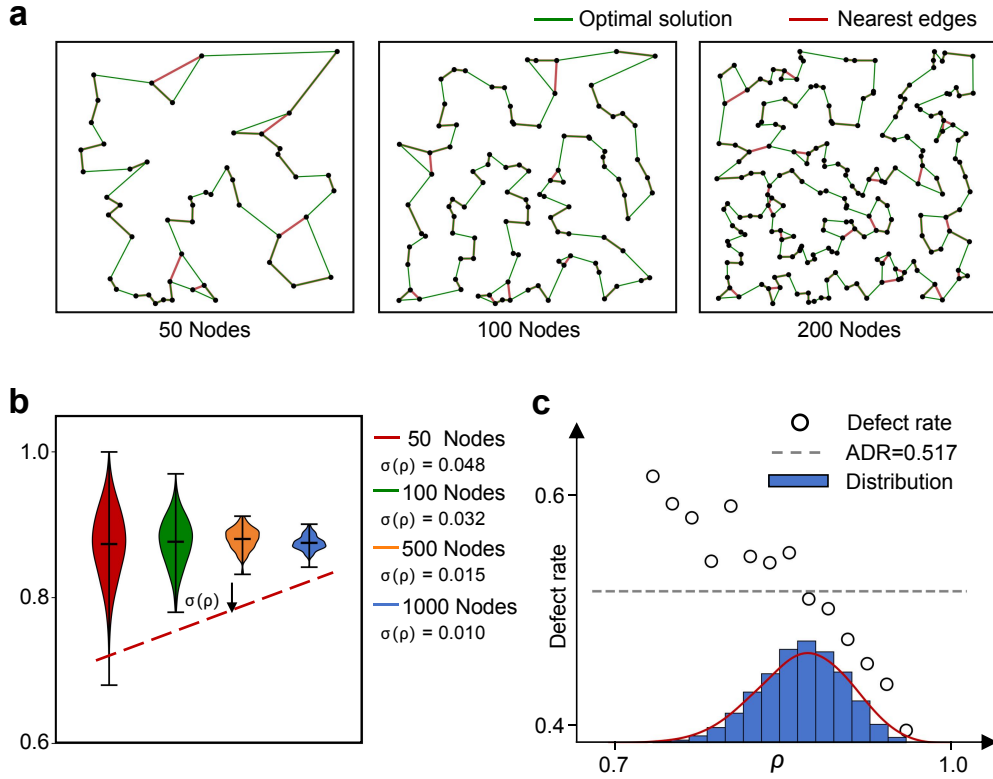


Figure 2: **(a)** The preference of the model’s solutions for nearest-neighbors at different node scales (50/100/200) generated from a uniform distribution. The green line represents the optimal solutions, while the red line represents the nearest-neighbor edges not covered by the optimal solutions. Most of the nearest-neighbor edges are included in the optimal solutions. **(b)** The statistical characteristics of nearest-neighbor density for instances with different node scales under the uniform distribution. As the node scale increases, the standard deviation decreases. **(c)** The model’s performance on instances with different nearest-neighbor densities under uniform distribution. Generally, the model performs better (worse) on instances with high (low) nearest-neighbor density.

3.2 Calculation of nearest-neighbor density under different distributions

3.2.1 Random uniform Euclidean (RUE) dataset

First, we evaluate the statistical results of the nearest-neighbor density on instances generated from the uniform distribution with the number of nodes varying from 20 to 50 in step 5. The nearest-neighbor density maintains a high level regardless of the node scale, indicating that each node is adjacent to its nearest neighbor on the optimal Hamiltonian circuit with a high probability. We observe an upward trend as the number of nodes increases on the RUE data (**Table 1**).

Table 1: The estimation of ρ_n for instances generated under different distributions

Node Size	The Nearest Density ρ_n		
	Uniform	Normal	Scale-free
20	0.8694	0.8538	0.7596
25	0.8685	0.8578	0.7504
30	0.8700	0.8601	0.7523
35	0.8709	0.8629	0.7493
40	0.8722	0.8645	0.7525
45	0.8727	0.8665	0.7620
50	0.8738	0.8695	0.7571

We analyze the aggregation degree of ρ_n as the number of nodes varies from 50 to 1000 (**Fig. 2b**) and observe that as the node size increases, the standard deviation of ρ_n decreases, indicating the convergence of ρ_n towards the $\mathbb{E}(\rho_n)$. This suggests that as the node size grows, the representativeness of instances generated by uniform distribution deteriorates.

Intuitively, a larger ρ_n of an instance indicates a lower difficulty. We test the performance of Transformer-TSP solver^[34] on the RUE test set with 10,000 samples of 50 nodes. We classify some samples as ‘defective’ based on the optimal gap and then calculate the defect rate for different instances (**Fig. 2c**). Specifically, we consider the optimal gap (defined as $\frac{\text{NN}(G)}{\text{OPT}(G)} - 1$) of the solution output $\text{NN}(G)$ by the Transformer-TSP solver on a specific instance G under the greedy decoding type. When the gap exceeds a threshold (i.e., 0.1% in this study), the solution is classified as ‘defective’. The defect rate refers to the proportion of defective solutions for the test instances. Generally, The model performs better (worse) on instances with high (low) nearest-neighbor density.

Based on the above experiments, we analyze the asymptotic bounds of the nearest-neighbor density ρ_n when $n \rightarrow \infty$.

Theorem 1. *Given the TSP instance $G = (V, E, b)$ on the two-dimensional Euclidean plane and $c_i = (x_i, y_i) \in V(G)$, where $(c_i)_{i=1}^{|V|} \sim \text{Uniform}([0, 1] \times [0, 1])$, the nearest-neighbor density ρ_n has an asymptotic lower bound $\rho_n \geq \frac{27-32\beta}{7}$, as $n \rightarrow \infty$, a.s..*

Remark 2. β is a known constant called the **Euclidean TSP Constant**. When placing n cities on a square of area $[0, 1] \times [0, 1]$. uniformly at random, the optimal tour length l_{opt} approaches the limit^[8]:

$$\lim_{n \rightarrow \infty} \frac{l_{\text{opt}}}{\sqrt{n}} = \beta. \text{ a.s.} \quad (3)$$

The best estimate for β is 0.7124^[15]. Thus our lower bound for ρ_n takes 0.6005 approximately. However, the theoretical upper bound estimation of the TSP constant for TSP remains an open problem. Currently, the best theoretical upper bound obtained is $\beta \leq 0.90304$.

According to our observation in **Table 1**, we propose the following conjecture.

Conjecture 2. *Given the TSP instance $G = (V, E, b)$ on the two-dimensional Euclidean plane and $c_i = (x_i, y_i) \in V(G)$, where $(c_i)_{i=1}^{|V|} \sim \text{Uniform}([0, 1] \times [0, 1])$, the following two statements hold*

1. $\mathbb{E}(\rho_n)$ increases with n .
2. $\rho_n \rightarrow_p \mathbb{E}(\rho_n)$, as $n \rightarrow \infty$, where $\mathbb{E}(\rho_n) > 0.87, n \rightarrow \infty$.

We can show that as the node size increases, the instances obtained from the uniform distribution probabilistic sampler become less representative (as reflected in the decreasing standard deviation of ρ_n with increasing node size (**Fig. 2b**). Moreover, this creates a simpler subproblem: when we deal with random uniform Euclidean instances, the greedy algorithm is not as bad as imagined, which is counterintuitive.

3.2.2 Random normal Euclidean (RNE) dataset

We also estimate ρ_n of normal Euclidean instances with the number of nodes varying between 20 and 50. According to **Table 1**, the nearest-neighbor density remains in a relatively high level (≥ 0.85).

3.2.3 TSPLib95 dataset

TSPLib95 is a well-known benchmark library^[25] of sample instances for TSP and related combinatorial optimization problems. In this part, we selected 38 instances from TSPLib95 (with node sizes less than 400 for computational convenience and the problem type is EUC_2D) to test their nearest-neighbor density (**Table 2**). The results show that some datasets have a nearest-neighbor density smaller than 0.85, indicating that the topological characteristics of the city datasets may not be approximated well by simple distributions. Notably, the ρ_n values for the two instances, a280 and pr107, are less than 0.8. We will discuss the potential patterns in such instances later.

Table 2: Real TSP datasets

Name	Node Size	ρ_n	Name	Node Size	ρ_n
eil51	51	0.8529	pr144	144	0.9583
berlin52	52	0.8077	ch150	150	0.8800
st70	70	0.8286	pr152	152	0.9342
eil76	76	0.8092	u159	159	0.9444
pr76	76	0.9211	rat195	195	0.9359
rat99	99	0.8485	d198	198	0.8283
KroA100	100	0.8700	KroA200	200	0.8550
KroB100	100	0.8700	KroB200	200	0.9200
KroC100	100	0.9100	ts225	225	0.8267
KroD100	100	0.8600	tsp225	225	0.8689
KroE100	100	0.9100	pr226	226	0.8842
rd100	100	0.8300	gil262	262	0.8779
eil101	101	0.8218	gil262	262	0.8798
lin105	105	0.9238	pr264	264	0.9564
pr107	107	0.7555	a280	280	0.7952
pr124	124	0.9556	pr299	299	0.8434
bier127	127	0.8674	pr299	299	0.8434
ch130	130	0.8615	lin318	318	0.9025
pr136	136	0.8161	rd400	400	0.8700

4 Data augmentation

4.1 TSP instances induced by scale-free network

Scale-free networks^[7] are a type of complex network characterized by a small number of highly connected nodes and many nodes with fewer connections. This structure follows a power-law degree distribution, i.e., $P(d) \propto d^{-\alpha}$. Scale-free networks are commonly found in various real-world systems, such as social networks, the internet, and biological networks^[6]. For the TSP, the topological structure of the nodes is trivial, and the metric information between nodes is critical. The nearest-neighbor distance is closely related to the nearest-neighbor density we proposed, and the nearest-neighbor distance reflects the local clustering feature of nodes. For example, in reality, the clustering feature in developed and underdeveloped areas is different, such as in the distribution map of town nodes in the United States (**Fig. 3a**). However, for the uniform euclidean distribution with node size n , the probability density function of the nearest-neighbor distance $P(r_1) \propto r(1 - \pi r^2)^{n-2}$,

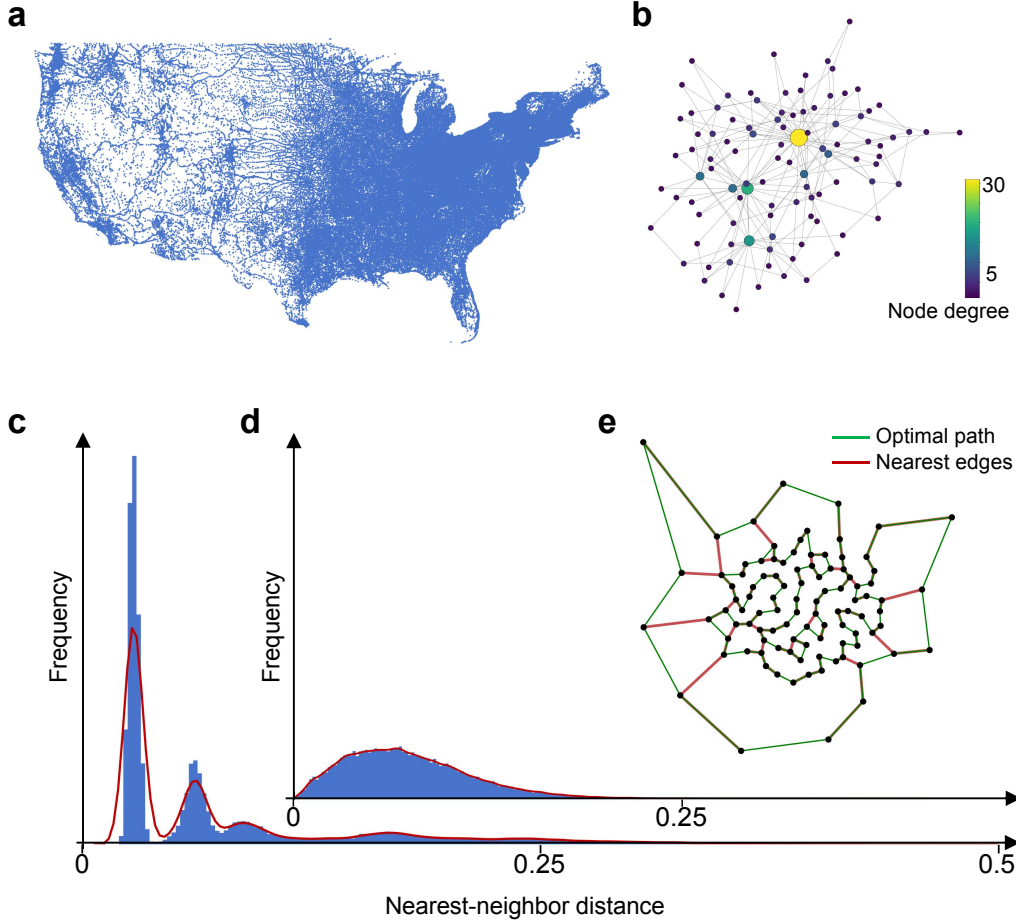


Figure 3: **(a)** Illustration of a TSP instance containing 115,475 towns in the United States from the USA TSP Challenge. **(b)** A scale-free network with 100 nodes generated using the Barabási-Albert model (Appendix A.5). **(c)** Distribution of nearest-neighbor distances for the TSP instances generated using Algorithm 1, exhibiting a multimodal distribution. **(d)** Distribution of nearest-neighbor distances for the traveling salesman problem instances generated using the uniform distribution. **(e)** Visualization of the instance with a size of 100 generated by Algorithm 1.

so the tail of the nearest-neighbor distance distribution decays rapidly especially when n is large (**Fig. 3d**).

In this paper, we first generate a scale-free network using the Barabási-Albert model^[11], then convert the degree features of the nodes into distance features. Specifically, it is manifested as points with higher nodes exerting a stronger attraction on neighboring nodes. Next, we use a spring layout algorithm^[10] to restore the node coordinates based on the distance information. Details can be found in **Algorithm 1**. Thus, the greater the node degree, the stronger its attraction, resulting in a radial distribution of nodes from the center to the periphery. In particular, we found that the nearest-neighbor distances follow a multimodal distribution in our case.

This indicates that the distribution of nodes exhibits a multilevel morphology in such cases with nodes closer to the center being denser and those closer to the edges being sparser. When addressing the TSP in this context, the model needs to be more *sophisticated* and cannot solely rely on nearest-neighbor distances, especially during hierarchical transitions from sparse regions to dense regions. As usual, we calculated the nearest-neighbor density ρ_n on this type of instances and found that it is lower compared to the instances discussed in the previous section (**Table 1**).

Algorithm 1 TSP-Instances Induced by Scale-Free Network

- 1: **Input:** Parameters for Barabási-Albert model, tunable constant k , the instance size n .
 - 2: Use the Barabási-Albert model to generate a scale-free network.
 - 3: **for** each pair of nodes u and v in the network **do**
 - 4: Let d_u and d_v be the degrees of nodes u and v respectively.
 - 5: Calculate the distance d_{uv} between nodes u and v : $d_{uv} = \exp(-k * (\deg(u) + \deg(v)))$ where k is a tunable positive constant.
 - 6: **end for**
 - 7: Use the spring layout algorithm to restore the position coordinates of the nodes based on distance information.
 - 8: **Output:** Obtain TSP instances where the nearest-neighbor distance follows a power law distribution.
-

4.2 Drilling problem instances

The drilling problem^[23] is an industrial optimization task to model the optimal path for drilling predetermined locations in mechanical manufacturing or electronic device production (e.g., circuit boards or mechanical parts). The objective is to minimize the distance or time for the drill head to move between drilling locations. These points often follow specific distribution patterns, reflecting practical production requirements and potentially displaying some regularity. Compared to general TSP instances sampled by the uniform distribution, where node layouts might be random or lack a specific arrangement, the points in the drilling problem are often associated with specific processes or product structures (e.g., a280.tsp in the TSPLIB dataset) (**Fig. 4a,b**).

It is easy to see that the nodes in the drilling problem instance exhibit a locally parallel grid-like layout, which often results in parallel line segments in the tour path (**Fig. 4a**). Similar examples are also frequently found in real-world city-based datasets. From the arrangement of shops along parallel streets to city layouts shaped by specific terrain or historical reasons, there can often be a relatively more regular grid-like structure.

Instances with grid-like patterns may seem relatively easy to address. If the spacing between two parallel grid segments is smaller than the spacing between points within each segment, the nearest-neighbor density will significantly decrease. We construct synthetic instances to demonstrate it. Specifically, we sample $\frac{n}{2}$ equally spaced points on each of the parallel lines $y = x$ and $y = x + 0.05$, where n is the size of the TSP instance. It is straightforward to calculate that the nearest-neighbor density on this constructed counterexample is $\rho_n = \frac{2}{n}$ when n is sufficiently large. We used several deep learning-based solvers on this type of data and found that the results were unsatisfactory (**Fig. 4c**).

4.3 Fine-tune the base solver with augmented instances

Utilizing the examples from the previous subsection as the basic construction instances, we create a perturbation-based instance augmentation algorithm and generate an instance set of 10000 sample instances with a node size of 50, where ρ_{50} spans values between 0.06 and 0.90 (**Fig. 5b**). The core idea is similar to stochastic offset data generation, where Gaussian perturbations of different scales are applied to the basic construction instances. The process generates instances along the transformation path from basic construction instances to RNE instances, which in turn results in samples with more diverse nearest neighbor density distributions (**Algorithm 2**).

We performed full fine-tuning on several classical neural solvers using augmented data (**Table 3**). It is worth noting that, without fine-tuning, these neural solvers showed varying degrees of performance decline on the constructed instances, with CycleFormer^[36] performing the worst. Compared with the base solvers, most solvers show performance improvements on the constructed instances such as the drilling model and scale-free model instances. Additionally, we observed that except for POMO, other neural solvers also achieved improvements on standard benchmarks (e.g., the RUE instances) after fine-tuning (The experimental details could refer to Appendix A.6).

To further explore the generality of our data augmentation method, we also tested the performance of solvers before and after fine-tuning on the synthetic instances presented in the previous work^[32], which adopt the convolution distribution of both uniform and normal distributions, resulting in

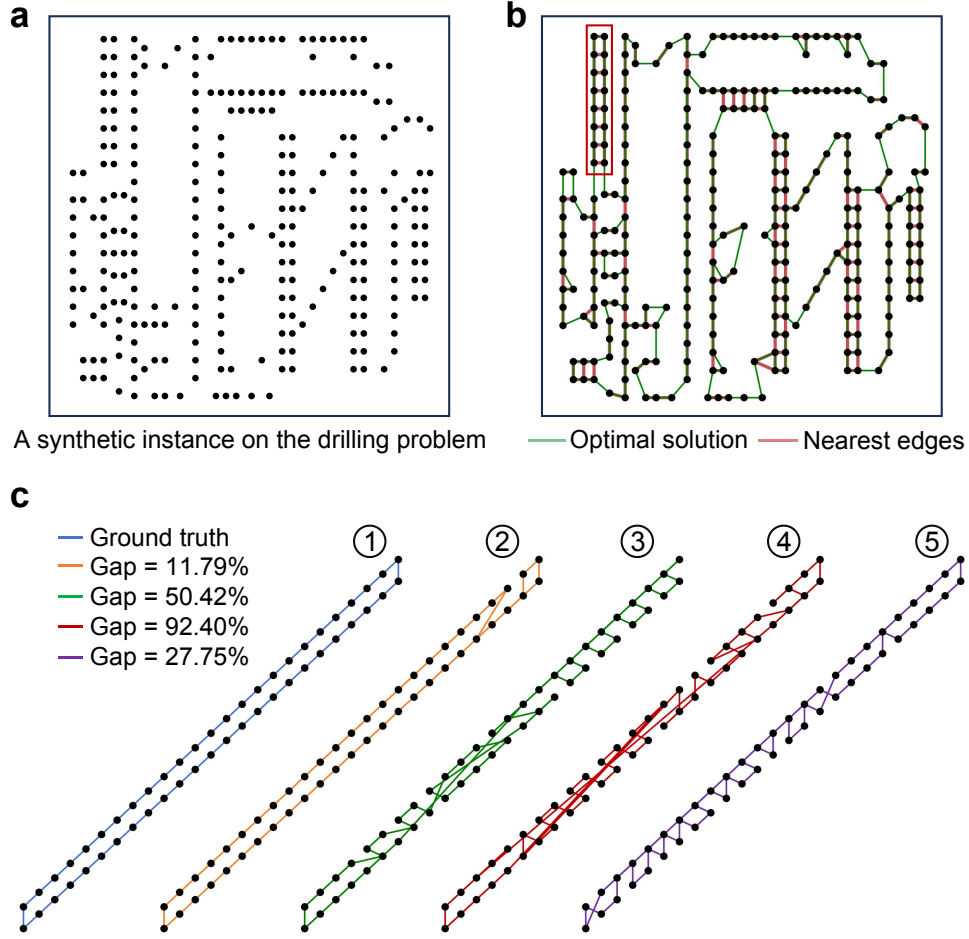


Figure 4: **(a)** Visualization of the a280 instance from TSPLIB. **(b)** The optimal solution derived from the a280 instance, where the green line represents the optimal solution, the red line represents the nearest-neighbor edges not covered by the optimal solution, and the orange highlights the parallel pattern layout observed in this type of instance. **(c)** The artificial instances constructed based on the pattern in the drilling problem with ① representing the exact solution and ②-⑤ indicating the solutions of TSP-GNN^[16], TSP-Transformer^[34], CycleFormer^[36], and the large-scale version of CycleFormer.

varying degrees of performance degradation for all solvers. However, after fine-tuning, we observed performance improvements for all solvers except TSP-GNN, with Transformer-TSP showing particularly significant gains—achieving performance improvements of 86% and 93% under the greedy decoding and beam search decoding concerning the optimal gap, respectively. This indicates that fine-tuning with augmented data enables solvers to capture essential features better when solving TSP.

Moreover, the experiments reveal that CycleFormer may suffer from severe overfitting issues in the RUE instances. Its performance was the worst among all solvers on drilling model and convolution distribution instances, though CycleFormer performs exceptionally well in the RUE instances. Even after fine-tuning, it failed to achieve notable improvements in the convolution distribution instances. We also observed that before fine-tuning, the larger version of CycleFormer outperforms the original CycleFormer on the RUE instances but performs much worse on the drilling model. This indicates that simply pursuing an increase in model size while ignoring data quantity or quality is unscientific, and ignoring dataset bias or solely focusing on improving benchmark performance during neural

Algorithm 2 Generate Perturbed Parallel Line Points with Rotation

- 1: **Input:** Total number of points n , large noise ratio α , small noise ratio β ,
 - 2: large noise standard deviation σ_{large} , small noise standard deviation σ_{small}
 - 3: **Output:** Set of perturbed points
 - 4: Randomly select a slope s and a distance d between two parallel lines and define two parallel lines on the $[0, 1] \times [0, 1]$ plane using s and d
 - 5: Generate $n/2$ equally spaced points on each line segment, and combine points from both lines to form a set of n points, denoted as \mathcal{P}
 - 6: Randomly select $\alpha \cdot n$ points from \mathcal{P} and apply large Gaussian noise with standard deviation σ_{large} and apply small Gaussian noise with standard deviation σ_{small} to the remaining $\beta \cdot n$ points
 - 7: Uniformly sample a rotation angle θ from $[0, 180]$ degrees and rotate all points in \mathcal{P} by angle θ
 - 8: **Return** the final set of rotated and perturbed \mathcal{P} .
-

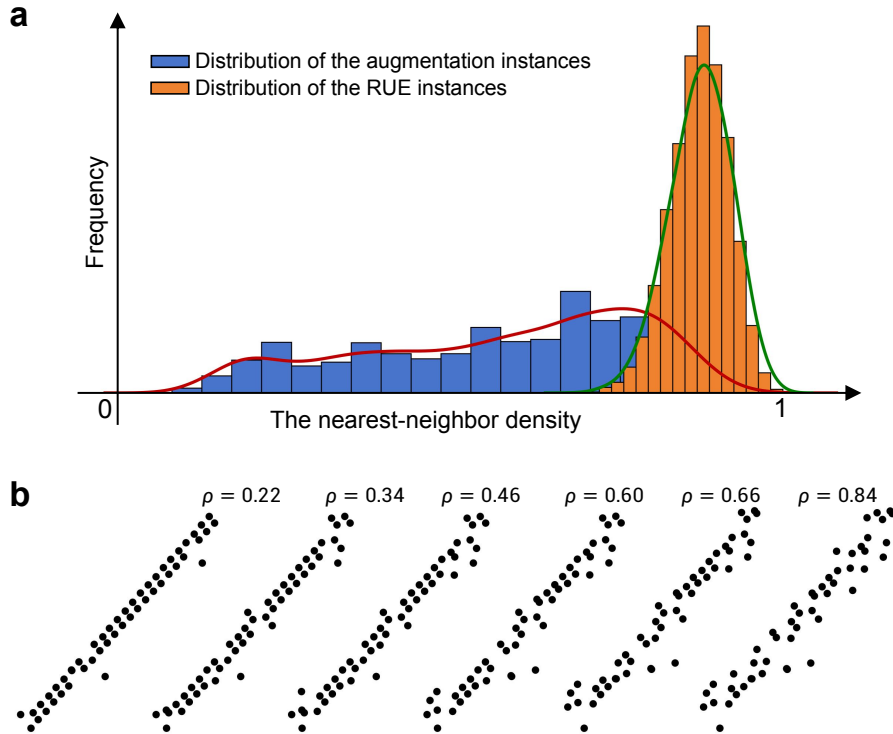


Figure 5: (a) Distribution of the nearest-neighbor density ρ_{50} for the augmented instances constructed by perturbing the drilling model instances. (b) Visualization of nine augmented instances with ρ_{50} ranging from 0.1 to 0.9.

solver training can lead to serious consequences that may not be hard to detect in ideal experimental environments.

5 Limitations of data-driven methods: Is augmentation all you need?

We have two problems to solve in this section.

1. **(About Data)** As mentioned earlier, we constructed two types of instances with low nearest-neighbor density, enhancing the robustness of the network as training data. However, the examples we constructed exhibit distinct characteristics. Are there other instances that are not covered by our construction?

Table 3: Results on the RUE, scale-free, drilling model and convolution distribution TSP Instances

Algorithm	Decoding Type	RUE		Scale-free Model		Drilling Model		Convolution Distribution	
		Length	Gap (%)	Length	Gap (%)	Length	Gap (%)	Length	Gap (%)
CONCORDE ^[2,3]	Exact	5.688	0	4.705	0	1.965	0	1.921	0
TSP-GNN ^[16]	Greedy	5.928	4.227	5.375	14.238	2.769	40.945	2.290	19.189
TSP-GNN (+DA)	Greedy	5.924	4.157	5.302	12.687	2.574	31.020	2.260	17.627
TSP-Transformer ^[34]	Greedy	5.702	0.248	4.844	2.968	2.540	29.838	2.495	30.730
TSP-Transformer (+DA)	Greedy	5.699	0.192	4.803	2.095	1.977	0.637	2.002	4.280
POMO ^[19]	Greedy	5.708	0.365	4.994	6.143	2.161	9.992	1.988	3.460
POMO (+DA)	Greedy	5.710	0.385	5.011	6.506	2.005	2.037	1.988	3.445
Pointerformer ^[14]	Greedy	5.709	0.371	5.044	7.212	2.572	30.933	2.396	24.722
Pointerformer (+DA)	Greedy	5.707	0.347	5.036	7.031	1.988	1.166	2.335	21.547
CycleFormer ^[36]	Greedy	5.723	0.593	5.317	13.008	3.344	70.228	3.319	72.752
CycleFormer (+DA)	Greedy	5.720	0.563	5.210	10.744	2.065	1.965	3.213	66.753
CycleFormer.Large ^[36]	Greedy	5.699	0.207	5.156	9.592	3.797	93.356	3.085	60.573
CycleFormer.Large (+DA)	Greedy	5.696	0.154	5.131	9.048	1.977	0.643	2.589	32.806
TSP-GNN ^[16]	Beam search	5.767	1.396	5.062	7.586	2.559	30.256	2.089	8.727
TSP-GNN (+DA)	Beam search	5.766	1.379	5.044	7.203	2.404	22.366	2.102	9.404
TSP-Transformer ^[34]	Beam search	5.689	0.027	4.756	1.089	2.336	19.322	2.382	24.867
TSP-Transformer (+DA)	Beam search	5.689	0.018	4.735	0.657	1.966	0.061	1.953	1.673
POMO ^[19]	Beam search	5.694	0.116	4.824	2.536	2.080	5.875	1.949	1.451
POMO (+DA)	Beam search	5.694	0.118	4.836	2.795	1.980	0.789	1.946	1.279
Pointerformer ^[14]	Beam search	5.693	0.100	4.807	2.160	2.226	13.326	2.177	13.292
Pointerformer (+DA)	Beam search	5.694	0.109	4.783	1.654	1.967	0.112	2.095	9.024
CycleFormer ^[36]	Beam search	5.691	0.056	4.793	1.864	2.604	32.531	2.980	55.127
CycleFormer (+DA)	Beam search	5.690	0.039	4.761	1.193	1.973	0.453	2.878	49.409
CycleFormer.Large ^[36]	Beam search	5.689	0.032	4.763	1.233	2.946	49.938	2.749	43.062
CycleFormer.Large (+DA)	Beam search	5.690	0.042	4.743	0.800	1.966	0.083	2.284	18.542

Note: All gaps (%) are calculated relative to the results from CONCORDE as the baseline. (+DA) refers to the base solvers fine-tuned on augmented data proposed by us. **Bold** text indicates performance gains after fine-tuning on the current instance set.

- (About Model) On uniform distribution, we seem to be able to obtain effective algorithms using neural network methods. However, this efficient algorithm for uniform distribution cannot cover all instances. Can we utilize different algorithms, i.e., ensemble methods, to cover all instances?

In the following, we present some (negative) results regarding the following two questions separately.

5.1 No efficient complete generator based on ρ

First, we need to clarify whether there are more general augmentation methods based on the nearest-neighbor density ρ_n , such as those using generative deep learning. Unfortunately, we will prove that any polynomial-time generative method is not complete. As a preparation, we first introduce several concepts of computational complexity^[27,35].

Definition 2 (Language). A language L is a set of strings. Every language L induces a binary classification task: the positive class contains all the strings in L , and the negative class contains all the strings in L 's complement L^C .

Definition 3 (Generator). A generator for a language L is a nondeterministic Turing machine. A generator is **complete** if it can generate every example: for every sufficiently large n , for every $w \in L$ of length n it holds that $w \in S_L(n)$. A generator S_L is called **efficient** if it runs in polynomial time.

Remark 3. The definition of generator implies generating both a sample w and its correct label ($w \in L$). One widely used efficient generator satisfies this definition which starts with a seed set of deterministically-labeled samples and applies class-preserving rewrites.

The following theorem indicates that for a generator for TSP instances based on ρ_n , only one of efficiency and completeness can be achieved.

Theorem 3. There is no efficient complete generator to generate the instances with the nearest-neighbor density $\rho_n \leq \delta$, where $\delta \in (0, 1)$, unless $NP = CoNP$.

As mentioned before, we can cover the range of nearest-neighbor density values by using **Algorithm 2**. However, according to **Theorem 3**, since **Algorithm 2** operates in polynomial time, it is still not complete. In other words, for a specific nearest-neighbor density value, there exist certain

combinatorial graph structures that cannot be generated by **Algorithm 2**. Moreover, there will not exist an efficient and complete sampler for nearest-neighbor density ρ , such as generating instances via neural networks.

5.2 No efficient algorithmic coverage

We have found that existing neural network algorithms perform excellently on the RUE TSP instances, at least when the problem scale is not particularly large. In this paper, we discover and confirm that learning-based solvers are biased. Nevertheless, is it possible to train solvers with different preferences for different problem scenarios and use ensemble methods to obtain a universal solver? We will explain that achieving this would at least require an exponential number of solvers in the ensemble unless $P = NP$.

Definition 4 (Efficient Algorithmic Coverage). *For a combinatorial optimization problem $\mathcal{P} \in NPC$, let n be the size of the instances, C be the set of all problem instances of size n , C_1, C_2, \dots, C_N are subsets of C , and $N = O(\text{poly}(n))$. For every C_i , there exists a corresponding efficient algorithm \mathcal{A}_i . If $\{C_i, \mathcal{A}_i\}_{i=1}^N$ satisfies the following properties:*

- (Completeness) $\bigcup_{i=1}^N C_i = C$ ensures that all instances are represented.
- (Effectiveness) $\forall x_i \in C_i, \frac{|\mathcal{A}(x_i) - \mathcal{A}^*(x_i)|}{\mathcal{A}^*(x_i)} \leq \epsilon$.
- (Independence) For all C_i , there exists $\tilde{x}_i \in C_i$, such that

$$\forall j \neq i, \frac{|\mathcal{A}_j(\tilde{x}_i) - \mathcal{A}^*(\tilde{x}_i)|}{|\mathcal{A}^*(\tilde{x}_i)|} > \epsilon,$$

where \mathcal{A}^* is the exact algorithm and ϵ is the approximation ratio.

then we denote $\{(C_i, \mathcal{A}_i)\}_{i=1}^N$ as the efficient algorithmic coverage for \mathcal{P} with instance size n .

Theorem 4. *There does not exist an exact efficient algorithmic coverage for $\mathcal{P} \in NPC$ unless $NP = P$.*

Theorem 5. *If the original problem $\mathcal{P} \in NPC$ does not have a polynomial-time approximation algorithm with the approximation ratio of ϵ , there does not exist an efficient algorithmic coverage with the approximation ratio of ϵ for \mathcal{P} .*

The above results are consistent with our previous discussion. From **Figure 2** and **Conjecture 2**, we know that the concentration of nearest-neighbor density in the uniform distribution instances increases as the number of nodes grows. This means that, from the perspective of nearest-neighbor density, the range of scenarios that the uniform distribution can cover becomes increasingly limited. Therefore, as the number of nodes increases, the number of specific solvers required for different instances will also grow. The results indicate that this growth is at least exponential.

6 Related works

The generalization ability of neural solvers. Existing learning-based solvers often struggle with generalization when faced with changes in problem distributions. Some studies have focused on creating new distributions^[31,37]. Zhang *et al.*^[37] defined the concept of hardness of TSP instance. However, the definition of hardness is solver-specific. We know this type of instance is difficult for some solvers, but do not understand why. Min *et al.* evaluated the solver-agnostic hardness of various distributions based on the parameter $\tau = l_{opt}/\sqrt{nA}$ defined in the reference^[11], where A denotes the area covered by the TSP instance, l_{opt} represents the length of the optimal solution and n is the number of cities. However, this complexity is only applicable to decision TSP, whose goal is to determine whether there exists a path whose total distance does not exceed a given threshold. Lischka *et al.*^[22] used different data distributions to train and test their solvers, but their data augmentation is based on the traditional mutation operators^[9]. They did not show why the learning solvers training on the uniform distribution dataset may fail. In this paper, we address this challenge by defining a statistic called *the nearest-neighbor density* that not only reflects the inherent learning difficulty of the samples but is also closely related to the solving process of prediction-based learning algorithms.

We believe it can better capture the greedy behavior in the learning-based solvers introduced by the training data.

The design of universal neural solvers. Can deep learning learn to solve any task? Yehuda *et al.*^[35] showed that any polynomial-time data generator for an NP-hard classification task will output data from an easier $\text{NP} \cap \text{coNP}$ task. However, their theoretical results only apply to data generators that provide labels. Methods that do not require labels, such as reinforcement learning, do not suffer from the problem above. Can we use reinforcement learning to train a universal solver? Wang *et al.*^[32] proposed an approach to address the generalization issues and provided a so-called ‘universal solver’ applied to a wide range of problems. However, they do not guarantee the so-called universality. A wider range of applications does not necessarily imply universality. Unfortunately, we will demonstrate that such an approach cannot yield a universal solver. The other potential solution to the generalization problem is to train different solvers in an ensemble manner^[12]. However, we will demonstrate that such an approach is computationally intensive (non-polynomial).

7 Conclusion

We introduced the nearest-neighbor density to describe the nearest-neighbor bias introduced by the training dataset (uniform distribution) in neural solvers for TSP. Extensive experiments thoroughly validated this. In particular, **conjecture 2** may serve as an intriguing open problem in the intersection of combinatorial optimization and probability theory.

We developed a data augmentation method based on nearest-neighbor density and real-world scenarios to alleviate the nearest-neighbor preference. Fine-tuning the base solver with these augmented instances significantly improved its generalization performance. However, this does not imply that we have achieved a universal solver. Data augmentation as a solution is not fundamental to address generalization challenges in combinatorial optimization problems. We analyze the limitations of data-driven methods, highlighting that achieving a universal neural solver through data augmentation (either manual or adaptive) or ensemble methods is infeasible, even for small-scale instances.

The challenge faced by deep learning models lies in handling corner cases, which is precisely a characteristic of combinatorial optimization problems. Therefore, pursuing a universal neural solver seems unrealistic. Focusing on real-world optimization tasks might be more meaningful than improving performance on unrepresentative benchmarks. Developing fair and appropriate benchmarks to evaluate neural solvers is one of our future research directions.

On the other hand, due to their lack of interpretability, neural networks are prone to shortcut learning—solving complex problems by capturing superficial features in the data. How to better design data representations or model architectures to reduce the network’s reliance on superficial features is another critical question for the fields of AI for combinatorial optimization or even AI for Science.

References

- [1] Réka Albert and Albert-László Barabási. Statistical mechanics of complex networks. *Reviews of modern physics*, 74(1):47, 2002.
- [2] David Applegate, Robert Bixby, Vašek Chvátal, and William Cook. *Finding cuts in the TSP (A preliminary report)*, volume 95. Citeseer, 1995.
- [3] David Applegate, Robert Bixby, William Cook, and Vasek Chvátal. On the solution of traveling salesman problems. 1998.
- [4] Tapan P Bagchi, Jatinder ND Gupta, and Chelliah Sriskandarajah. A review of tsp based approaches for flowshop scheduling. *European Journal of Operational Research*, 169(3):816–854, 2006.
- [5] Pouya Baniasadi, Mehdi Foumani, Kate Smith-Miles, and Vladimir Ejov. A transformation technique for the clustered generalized traveling salesman problem with applications to logistics. *European Journal of Operational Research*, 285(2):444–457, 2020.

- [6] Albert-László Barabási. Scale-free networks: a decade and beyond. *science*, 325(5939):412–413, 2009.
- [7] Albert-László Barabási and Réka Albert. Emergence of scaling in random networks. *science*, 286(5439):509–512, 1999.
- [8] John H. Halton Beardwood Jillian and John Michael Hammersley. The shortest path through many points. *Mathematical proceedings of the Cambridge philosophical society*, 55(4), 1959.
- [9] Jakob Bossek, Pascal Kerschke, Aneta Neumann, Markus Wagner, Frank Neumann, and Heike Trautmann. Evolving diverse tsp instances by means of novel and creative mutation operators. In *Proceedings of the 15th ACM/SIGEVO conference on foundations of genetic algorithms*, pages 58–71, 2019.
- [10] Thomas MJ Fruchterman and Edward M Reingold. Graph drawing by force-directed placement. *Software: Practice and experience*, 21(11):1129–1164, 1991.
- [11] Ian P Gent and Toby Walsh. The tsp phase transition. *Artificial Intelligence*, 88(1-2):349–358, 1996.
- [12] Francisco J Gil-Gala, Marko Durasević, María R Sierra, and Ramiro Varela. Evolving ensembles of heuristics for the travelling salesman problem. *Natural Computing*, 22(4):671–684, 2023.
- [13] Michael Held and Richard M Karp. A dynamic programming approach to sequencing problems. *Journal of the Society for Industrial and Applied mathematics*, 10(1):196–210, 1962.
- [14] Yan Jin, Yuandong Ding, Xuanhao Pan, Kun He, Li Zhao, Tao Qin, Lei Song, and Jiang Bian. Pointerformer: Deep reinforced multi-pointer transformer for the traveling salesman problem. In *Proceedings of the AAAI Conference on Artificial Intelligence*, volume 37, pages 8132–8140, 2023.
- [15] Lyle A. McGeoch Johnson David S. and Edward E. Rothberg. Asymptotic experimental analysis for the held-karp traveling salesman bound. *roceedings of the 7th Annual ACM-SIAM Symposium on Discrete Algorithms*, 341, 1996.
- [16] Chaitanya K Joshi, Quentin Cappart, Louis-Martin Rousseau, and Thomas Laurent. Learning the travelling salesperson problem requires rethinking generalization. *Constraints*, 27(1):70–98, 2022.
- [17] Jared Kaplan, Sam McCandlish, Tom Henighan, Tom B. Brown, Benjamin Chess, Rewon Child, Scott Gray, Alec Radford, Jeffrey Wu, and Dario Amodei. Scaling laws for neural language models, 2020.
- [18] Wouter Kool, Herke Van Hoof, and Max Welling. Attention, learn to solve routing problems! *arXiv preprint arXiv:1803.08475*, 2018.
- [19] Yeong-Dae Kwon, Jinho Choo, Byoungjip Kim, Iljoo Yoon, Youngjune Gwon, and Seungjai Min. Pomo: Policy optimization with multiple optima for reinforcement learning. *Advances in Neural Information Processing Systems*, 33:21188–21198, 2020.
- [20] Pedro Larranaga, Cindy M. H. Kuijpers, Roberto H. Murga, Inaki Inza, and Sejla Dizdarevic. Genetic algorithms for the travelling salesman problem: A review of representations and operators. *Artificial intelligence review*, 13:129–170, 1999.
- [21] Yann LeCun, Yoshua Bengio, and Geoffrey Hinton. Deep learning. *nature*, 521(7553):436–444, 2015.
- [22] Attila Lischka, Jiaming Wu, Rafael Basso, Morteza Haghiri Chehreghani, and Balázs Kulcsár. Less is more-on the importance of sparsification for transformers and graph neural networks for tsp. *arXiv preprint arXiv:2403.17159*, 2024.
- [23] Godfrey C Onwubolu, BV Babu, and Godfrey C Onwubolu. Optimizing cnc drilling machine operations: traveling salesman problem-differential evolution approach. *New optimization techniques in engineering*, pages 537–565, 2004.

- [24] Ted K Ralphs, Leonid Kopman, William R Pulleyblank, and Leslie E Trotter. On the capacitated vehicle routing problem. *Mathematical programming*, 94:343–359, 2003.
- [25] Gerhard Reinelt. Tsplib95. *Interdisziplinäres Zentrum für Wissenschaftliches Rechnen (IWR), Heidelberg*, 338:1–16, 1995.
- [26] Daniel Rosenkrantz, Richard Stearns, and Philip II. An analysis of several heuristics for the traveling salesman problem. *SIAM J. Comput.*, 6:563–581, 09 1977.
- [27] Laura A. Sanchis. On the complexity of test case generation for np-hard problems. *Information Processing Letters*, 36(3):135–140, 1990.
- [28] Jingyan Sui, Shizhe Ding, Xulin Huang, Yue Yu, Ruizhi Liu, Boyang Xia, Zhenxin Ding, Liming Xu, Haicang Zhang, Chungong Yu, and Dongbo Bu. A survey on deep learning-based algorithms for the traveling salesman problem. *Frontiers of Computer Science*, 19(6):196322, 2025.
- [29] Oriol Vinyals, Meire Fortunato, and Navdeep Jaitly. Pointer networks. *Advances in neural information processing systems*, 28, 2015.
- [30] Ton Volgenant and Roy Jonker. A branch and bound algorithm for the symmetric traveling salesman problem based on the 1-tree relaxation. *European Journal of Operational Research*, 9(1):83–89, 1982.
- [31] Chenguang Wang, Yaodong Yang, Oliver Slumbers, Congying Han, Tiande Guo, Haifeng Zhang, and Jun Wang. A game-theoretic approach for improving generalization ability of tsp solvers. *arXiv preprint arXiv:2110.15105*, 2021.
- [32] Chenguang Wang, Zhouliang Yu, Stephen McAleer, Tianshu Yu, and Yaodong Yang. Asp: Learn a universal neural solver! *IEEE Transactions on Pattern Analysis and Machine Intelligence*, 2024.
- [33] Ou Wu and Rujing Yao. Data optimization in deep learning: A survey, 2023.
- [34] Bresson Xavier and Thomas Laurent. The transformer network for the traveling salesman problem. *arXiv preprint arXiv:2103.03012*, 2021.
- [35] Gal Yehuda, Moshe Gabel, and Assaf Schuster. It’s not what machines can learn, it’s what we cannot teach. In *International conference on machine learning*, pages 10831–10841. PMLR, 2020.
- [36] Jieun Yook, Junpyo Seo, Joon Huh, Han Joon Byun, and Byung-ro Moon. Cycleformer: Tsp solver based on language modeling. *arXiv preprint arXiv:2405.20042*, 2024.
- [37] Zeyang Zhang, Ziwei Zhang, Xin Wang, and Wenwu Zhu. Learning to solve travelling salesman problem with hardness-adaptive curriculum. In *Proceedings of the AAAI Conference on Artificial Intelligence*, volume 36, pages 9136–9144, 2022.

A Appendix

A.1 Proof of Theorem 1

Proof. According to the Remark 1, we know for the uniform distribution, the calculation of ρ_n simplifies to a specific form

$$\rho_n^* = \sum_{c_i \in V} \frac{I(c_i)}{n}.$$

Let r_k denote the distance from a given reference point to its k -th nearest-neighbor. For an instance with n nodes, a proportion ρ_n of the nodes are connected to their nearest-neighbors on the optimal hamiltonian tour. Therefore, the lower bound for the edges associated with these $\rho_n \cdot n$ nodes is given by:

$$\frac{1}{2} \rho_n \cdot n(r_1 + r_2) + \theta_1, \quad (4)$$

while the lower bound for the edges associated with the other nodes is given by:

$$\frac{1}{2} \rho_n \cdot n(r_2 + r_3) + \theta_2, \quad (5)$$

where θ_1 and θ_2 represent the deviation.

Therefore, we need to figure out the statistical distribution of the k -nearest-neighbor distances.

For a given reference point the absolute probability of finding its k -th neighbour ($k < n$) at a distance between r_k and $r_k + dr_k$ from it is given by the probability that out of the $n - 1$ random points (other than the reference point) distributed uniformly within the hypersphere of unit volume, exactly $k - 1$ points lie within a concentric hypersphere of radius r_k and at least one of the remaining $n - k$ points lie within the shell of internal radius r_k and thickness dr_k . Therefore,

$$P(r_k)dr_k = \binom{n-1}{k-1} V_k^{k-1} \sum_{q=1}^{n-k} \binom{n-k}{q} (1 - V_k)^{n-k-q} (dV_k)^q, \quad (6)$$

and $\mathbb{E}(r_k) = \int_0^R r_k P(r_k)$, where R is the radius of the D -dimensional hypersphere of unit volum.

Thus, we have

$$\begin{aligned} \mathbb{E}(r_k) &= \frac{\Gamma(\frac{D}{2} + 1)^{\frac{1}{D}}}{\sqrt{\pi}} \binom{n-1}{k-1} (n-k) \int_0^1 V_k^{k+\frac{1}{D}-1} (1 - V_k)^{n-k-1} dV_k \\ &= \frac{\Gamma(\frac{D}{2} + 1)^{\frac{1}{D}}}{\sqrt{\pi}} \binom{n-1}{k-1} (n-k) B(k + \frac{1}{D}, n-k) \\ &= \frac{\Gamma(\frac{D}{2} + 1)^{\frac{1}{D}}}{\sqrt{\pi}} \frac{\Gamma(k + \frac{1}{D})}{\Gamma(k)} \frac{\Gamma(n)}{\Gamma(n + \frac{1}{D})}, \end{aligned} \quad (7)$$

and

$$\begin{aligned} \mathbb{E}(r_k^2) &= \frac{\Gamma(\frac{D}{2} + 1)^{\frac{2}{D}}}{\pi} \binom{n-1}{k-1} (n-k) B(k + \frac{2}{D}, n-k) \\ &= \frac{\Gamma(\frac{D}{2} + 1)^{\frac{2}{D}}}{\pi} \frac{\Gamma(k + \frac{2}{D})}{\Gamma(k)} \frac{\Gamma(n)}{\Gamma(n + \frac{2}{D})}. \end{aligned} \quad (8)$$

When taking $D = 2$ and using Stirling's approximation, we get $\mathbb{E}(r_k) = \frac{1}{\sqrt{n\pi}} \frac{\Gamma(k + \frac{1}{2})}{\Gamma(k)}$ and $\mathbb{E}(r_k^2) = \frac{1}{n\pi} \frac{\Gamma(k + \frac{2}{2})}{\Gamma(k)}$. Let $r_{k,1}, \dots, r_{k,n}$ be n identically distributed copies of the random variable r_k , thus

$$\mathbb{E}[\|\sqrt{\frac{1}{n}} \sum_{i=1}^n r_{k,i} - \sqrt{n} \mathbb{E}(r_k)\|] = O(\frac{1}{n}).$$

Given that $\lim_{n \rightarrow \infty} \frac{l_{\text{opt}}}{\sqrt{n}} = \beta$ and $\lim_{n \rightarrow \infty} \frac{1}{2} \sqrt{\frac{1}{n}} \cdot [\rho_n \sum_{i=1}^n (r_{1,i} + r_{2,i}) + (1 - \rho_n) \sum_{i=1}^n (r_{2,i} + r_{3,i})] \leq \beta$, a.s.,

we have

$$\lim_{n \rightarrow \infty} \frac{5}{8} \rho_n + \frac{27}{32} (1 - \rho_n) \leq \beta, \text{ a.s.}$$

and we then concluded that $\rho_n \geq \frac{27-32\beta}{7}$ a.s., as $n \rightarrow \infty$. □

A.2 Proof of Theorem 3

Proof. Define the language L as follows: Given an instance I of the two-dimensional Euclidean TSP and a value $\delta \in (0, 1)$, if $\rho(I) \leq \delta$, then $I \in L$. Otherwise $I \in L^c$. L is NP-hard because it depends on solving the TSP itself. And the classification task $T(L)$ introduced by L is NP-hard, i.e., given an instance I , decide if $I \in L$.

Assume that there exists an efficient complete sampler S_L for L . Since L is complete, the classification task $T(S_L)$ induced by S_L , i.e., given an instance I generated by S_L , determine if $I \in L$, is equal to the task $T(L)$ introduced by L . Given a I generated by S_L , and $I \in L$, let sq be the sequence of random bits used by S_L to generate I . Since S_L runs in polynomial time, it must use at most polynomial number of random bits. Then $\forall I \in S_L$, there exists a string sq with length polynomial in $|I|$. Therefore a deterministic Turing machine that given I and sq can verify in polynomial time if $I \in L$. So $T(S_L) \in NP$. Similarly, we can show that $T(S_L) \in coNP$. Thus $T(S_L) \in NP \cap coNP$. Then, we have $T(L) \in NP \cap coNP$. However, $T(L) \in NP - \text{hard}$, and if $T(L) \in NP \cap coNP$, then $NP = coNP$. This leads to a contradiction. □

A.3 Proof of Theorem 4

Proof. Using proof by contradiction, assume that the efficient algorithm covering exists. We can simply obtain a polynomial-time exact solving algorithm by sequentially running \mathcal{A}_i . Then $\mathcal{P} \in P$. Since $P \in NPC$, this would imply $P = NP$, which is a contradiction. □

A.4 Proof of Theorem 5

Proof. The proof idea follows the proof of Theorem 4. □

A.5 Introduction to Barabási-Albert Model

The Barabási-Albert model is a fundamental framework for generating scale-free networks characterized by growth and preferential attachment. This model, also referred to as the scale-free model, operates as follows:

Initially, the network consists of m_0 nodes, connected arbitrarily, ensuring each node has at least one link. The network evolves through two primary mechanisms:

- **Growth.** At each time step, a new node is introduced to the network with m (where $m \leq m_0$) links. These links connect the new node to m existing nodes in the network.
- **Preferential Attachment.** The probability $P(k_i)$ that a new node will connect to an existing node i is proportional to the degree k_i of node i . This probability is given by:

$$P(k_i) = \frac{k_i}{\sum_j k_j}.$$

Preferential attachment is a probabilistic process, allowing new nodes to connect to any existing node, regardless of whether it is a highly connected hub or a node with few links.

This model effectively captures the dynamics of real-world networks, where new nodes tend to connect to already well-connected nodes, leading to a scale-free topology.

A.6 Experimental Details

We use the model by Bresson et al.^[34] as the base solver. It is a Transformer-based architecture. The transformer is learned by reinforcement learning. Hence, no TSP solutions/approximations are required. The solver has quadratic complexity $O(n^2L)$, where L is the depth of the models. Details of the network architecture and training process are provided in **Table S1**.

The base solvers involved in the comparison all have open-source model parameters. The decoding type of beam search is with the beam width uniformly set to 1000. During fine-tuning, we replaced one-fourth of the original training set (uniformly distributed) with sample instances constructed using the drilling model examples. The number of fine-tuning steps for different solvers is provided in **Table S1**. It should be noted that for POMO^[19] and Pointerformer^[14], the authors adopted an optional unit square transformations scheme during the inference phase. We omitted this step during comparisons to ensure fairness with other models.

The RUE test set contains 1280 instances with the node size of 50, derived from the test set used in prior works^[29,36]. However, we have revised the exact solutions for this test set. For the other two types of instances with a node size of 50, we have used our own generated datasets, each consisting of 1000 instances.

Table S1: Details of the neural network architecture and training process

Base Solver	Batch Size	Total TSP samples for training (fine-tuning)
TSP-GNN	512	1.28×10^7 (6.40×10^6)
TSP-Transformer	512	2.08×10^9 (1.28×10^7)
POMO	128	2.00×10^8 (1.28×10^7)
Pointerformer	64	3.00×10^8 (1.28×10^7)
Cycleformer	80	1.50×10^8 (4.00×10^6)

A.7 Convolutional distribution Instances

Wang *et al.* proposed a new method called ASP^[32]: Adaptive Staircase Policy Space Response Oracle (PSRO), which aims to address the generalization issues faced by previous neural solvers and provide a "universal neural solver" that can be applied to a wide range of problem distributions and scales. They generate data by randomly sampling $x \in \mathbb{R}^2$ from the unit square, and sampling $y \in \mathbb{R}^2$ from $N(0, \Sigma)$ where $\Sigma \in \mathbb{R}^{2 \times 2}$ is a diagonal matrix whose elements are sampled from $[0, \lambda]$ and $\lambda \sim U(0, 1)$. Next, a two-dimensional coordinate is generated by $z = x + y$. This describes a convolutional distribution which is the convolution of the uniform distribution and the Gaussian distribution.

We analyzed the nearest-neighbor density of these instances and found that they did not exhibit significantly low-density characteristics (**Table S2**). Interestingly, however, compared to a uniform distribution, there was indeed a noticeable decrease. This further demonstrates the effectiveness of our metric in evaluating the difficulty of instances for neural solvers. Additionally, we visualized some of the instances (**Fig. S1**), and interestingly, their distributions revealed regions of both sparsity and density. This closely resembles the examples we constructed based on scale-free complex networks.

Table S2: The estimation of nearest density ρ_n for adversarial instances

Node Size	The Nearest Density ρ_n Adversarial Instances
20	0.8506
30	0.8602
40	0.8619
50	0.8642

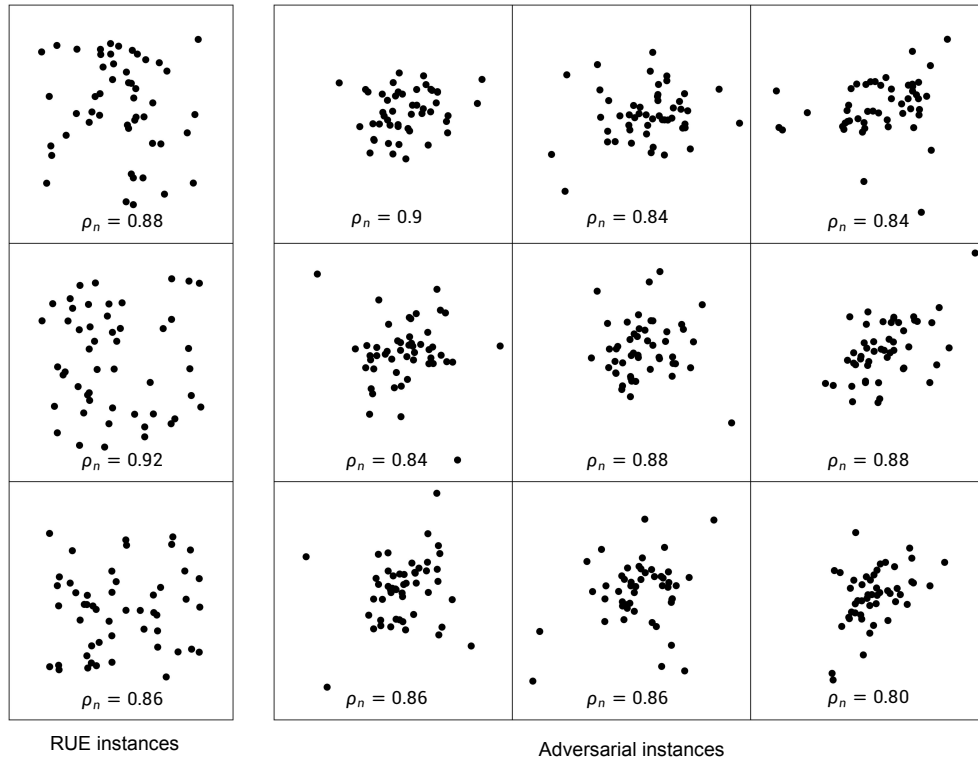


Figure S1: Visualization of some adversarial instances